

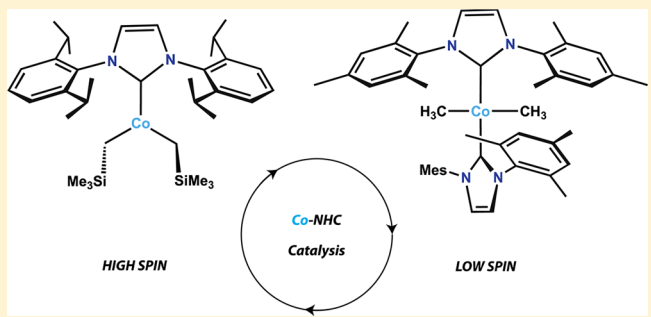
# NHC Complexes of Cobalt(II) Relevant to Catalytic C–C Coupling Reactions

Jacob A. Przyowski, Hadi D. Arman, and Zachary J. Tonzetich\*

Department of Chemistry, University of Texas at San Antonio, San Antonio, Texas 78249, United States

## Supporting Information

**ABSTRACT:** Alkyl compounds of cobalt(II) containing aryl-substituted N-heterocyclic carbene ligands have been prepared by reaction of the precursor chloro complexes  $[\text{CoCl}_2(\text{IMes})_2]$  and  $[\text{Co}_2\text{Cl}_2(\mu\text{-Cl})_2(\text{IPr})_2]$  (IMes = 1,3-dimesitylimidazol-2-ylidene; IPr = 1,3-bis(2,6-diisopropylphenyl)imidazol-2-ylidene) with Grignard reagents. Examples of alkyl complexes possessing both four-coordinate and three-coordinate geometries are reported. The chloro complex  $[\text{CoCl}_2(\text{IMes})_2]$  adopts a pseudotetrahedral geometry displaying an  $S = 3/2$  ground state, whereas the alkyl complex  $[\text{Co}(\text{CH}_3)_2(\text{IMes})_2]$  adopts a square-planar geometry consistent with an  $S = 1/2$  ground state. In contrast to  $[\text{Co}(\text{CH}_3)_2(\text{IMes})_2]$ ,  $[\text{Co}(\text{CH}_2\text{SiMe}_3)_2(\text{IPr})]$  exhibits a three-coordinate trigonal-planar geometry displaying an  $S = 3/2$  ground state. The catalytic efficacy of  $[\text{CoCl}_2(\text{IMes})_2]$  in Kumada couplings is examined, as is the chemistry of the alkyl complexes toward CO. The structure and reactivity of these compounds is discussed in the context of C–C coupling reactions catalyzed by cobalt NHCs.



## INTRODUCTION

N-heterocyclic carbenes (NHCs) are finding increased use as supporting ligands in early to mid first-row transition-metal chemistry for a variety of applications, from catalysis<sup>1</sup> to small-molecule activation<sup>2</sup> and biomimetic chemistry.<sup>3–6</sup> Iron NHC complexes, in particular, have received a great deal of attention, as evidenced by the growing number of reports in recent years.<sup>7</sup> Much of this interest stems from the documented success of iron NHC catalysts in C–C coupling reactions.<sup>8–13</sup> In addition to iron, NHC complexes of other earth-abundant metals such as cobalt are equally compelling as potential catalysts for a variety of organic transformations.<sup>14,15</sup> In this regard, several recent reports have highlighted the efficacious role of NHC coligands in C–C coupling reactions catalyzed by divalent cobalt salts.<sup>16–20</sup> Furthermore, the structural homology between many coordination complexes of Fe(II) and Co(II) suggests that the corresponding organometallic compounds containing NHC ligands may demonstrate similar parallels. The extent to which this homology can be extended to mechanisms of catalytic reactions involving organometallic iron and cobalt species is of great interest, considering that many such mechanisms involving these metals are as yet poorly understood. Previous work with iron by our laboratory<sup>21</sup> and others<sup>10,22–26</sup> has established that a variety of geometries and coordination numbers are possible for iron complexes containing simple monodentate NHC ligands. We were therefore curious as to whether similar structures and reactivity would be found for cobalt.

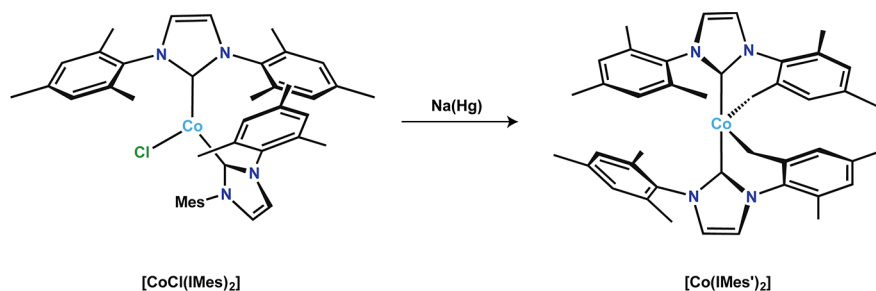
Among the transition metals, cobalt displays a very modest number of examples of NHC complexes.<sup>1</sup> Older reports have

described a variety of Co(I) and Co(0) compounds featuring NHC ligands.<sup>27–34</sup> Owing to the low formal oxidation state of Co in these compounds, each example features very strong field supporting ligands such as CO and Cp<sup>−</sup>. Higher oxidation state complexes of cobalt have also been prepared by employing chelating NHC variants.<sup>2,35–39</sup> Such compounds have been shown to demonstrate unique reactivity in certain instances<sup>40–43</sup> but are most likely unrelated to possible intermediates in C–C coupling reactions catalyzed by cobalt.

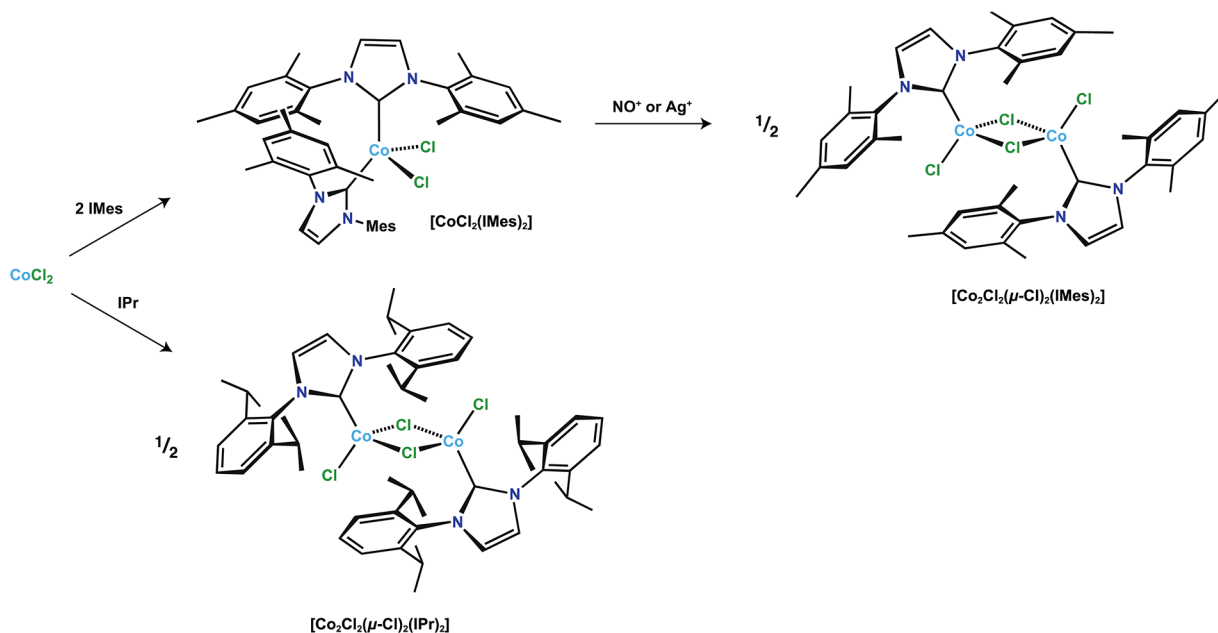
More recently, several examples of cobalt complexes featuring simple monodentate NHC ligands have been reported. Holm and Deng prepared a series of sulfide-bridged tetracobalt cubane structures employing alkyl-substituted NHC ligands, including an example of a monomeric Co(II) NHC thiolate complex.<sup>44</sup> Deng and co-workers have also described a series of homoleptic square-planar Co(I) and Co(II) complexes featuring similar alkyl-substituted NHC ligands, which were prepared by ligand displacement from  $[\text{Co}^{\text{I}}\text{Cl}(\text{PPh}_3)_3]$ .<sup>45</sup> These compounds were found to exhibit chemically reversible one-electron transfer, allowing for efficient homocoupling of Grignard reagents. Subsequent work by the same group described the synthesis and reactivity of  $[\text{Co}^{\text{I}}\text{Cl}(\text{IMes})_2]$ , also prepared from  $[\text{Co}^{\text{I}}\text{Cl}(\text{PPh}_3)_3]$ .<sup>46</sup> Reduction of this complex resulted in an unstable Co(0) species that was found to C–H activate at the *o*-methyl position of the IMes ligand, leading to a Co(II) dialkyl complex featuring two activated IMes ligands (IMes<sup>′</sup>; Scheme 1). Not extensively examined in the recent

Received: November 8, 2012

Scheme 1



Scheme 2



report by Deng was the corresponding chemistry of Co(II) species featuring the IMes ligand. In other work, Danopoulos and co-workers described the preparation of three-coordinate Co(II) species featuring the IPr ligand via aminolysis of  $[\text{Co}\{\text{N}(\text{SiMe}_3)_2\}_2]$  with  $\text{IPr}\cdot\text{HCl}$ .<sup>22</sup> Matsubara and co-workers reported similar species, including the dimeric Co(II) chloro complex  $[\text{Co}_2\text{Cl}_2(\mu\text{-Cl})_2(\text{IPr})_2]$ .<sup>47</sup> This species was demonstrated to serve as a precatalyst for several C–C couplings. Cleavage of the dimer to monomeric four-coordinate complexes was accomplished by addition of suitable bases such as pyridines. Such reactivity is very similar to that reported for the analogous iron(II) halide dimers containing the IPr ligand,<sup>21</sup> again highlighting similarities between the two systems. Absent in previous work with Co(II) NHCs is an examination of their stoichiometric reactivity with Grignard reagents to give alkyl complexes. The chemistry of these species may offer clues into the mechanism of coupling reactions catalyzed by Co(II) salts in the presence of NHC coligands. With these aims in mind, we set out to examine the chemistry of Co(II) complexes containing aryl-substituted NHC ligands.

## RESULTS AND DISCUSSION

**Halide Complexes.** As an entry point into the cobalt(II) chemistry, we targeted  $[\text{CoCl}_2(\text{IMes})_2]$  as a suitable starting material, in a fashion similar to our previous work with iron.<sup>21</sup> Addition of 2 equiv of IMes to anhydrous  $\text{CoCl}_2$  in THF

solvent afforded a deep blue solution from which a blue solid was isolated after recrystallization from toluene (Scheme 2). The NMR spectrum of the material indicated a paramagnetic complex but was too severely broadened at 20 °C to provide detailed structural information. Warming to 75 °C resulted in a sharpened spectrum (see the Supporting Information (SI), Figure S1), supporting the formulation of the compound as  $[\text{CoCl}_2(\text{IMes})_2]$ . The reason for the broadened spectrum at room temperature is unknown at this time. The analogous iron complex displays a relatively sharp spectrum at room temperature, but the bond distances in the cobalt compound are slightly shorter (*vide infra*), possibly accounting for more hindered bond movements at lower temperatures. Equilibrium between a monomeric and dimeric species is also possible; however, we observe no free ligand by NMR spectroscopy at reduced temperatures to support this proposal. Furthermore, solution magnetic susceptibility measurements of the material gave a magnetic moment of 3.9(1)  $\mu_{\text{B}}$ , also consistent with a monomeric high-spin  $S = 3/2$  complex. Identical reactions with the bulkier IPr ligand afforded the dimeric species  $[\text{Co}_2(\mu\text{-Cl})_2\text{Cl}_2(\text{IPr})_2]$ , in agreement with the results published by Matsubara (Scheme 2).<sup>47</sup> Both  $[\text{CoCl}_2(\text{IMes})_2]$  and  $[\text{Co}_2(\mu\text{-Cl})_2\text{Cl}_2(\text{IPr})_2]$  are deep blue crystalline solids that show the expected three ligand field transitions for a tetrahedral high-spin Co(II) ion (Figure S2, SI). The aggregation behavior of the compounds with respect to the steric bulk of the IMes and IPr

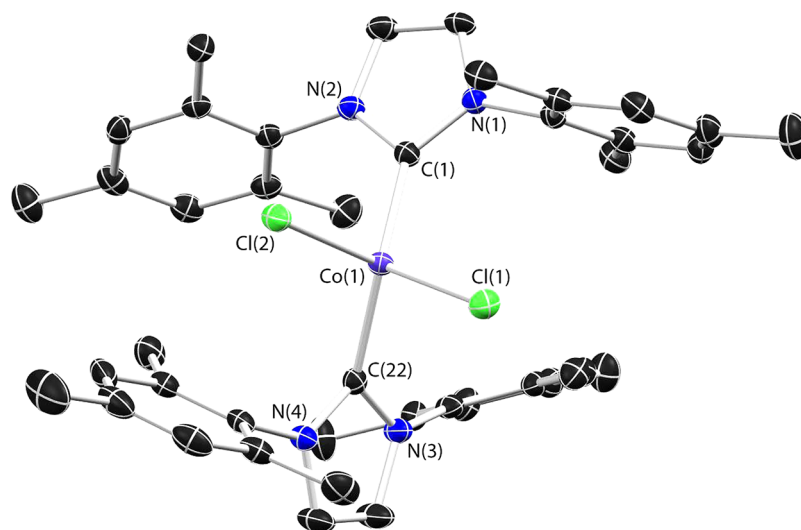


**Figure 1.** Thermal ellipsoid drawing (50%) of  $[\text{CoCl}_2(\text{IMes})_2]$ . Hydrogen atoms and the cocrystallized benzene molecule are omitted for clarity. Selected bond lengths ( $\text{\AA}$ ) and angles (deg):  $\text{Co}(1)\text{--C}(1) = 2.069(2)$ ,  $\text{Co}(1)\text{--C}(22) = 2.089(2)$ ,  $\text{Co}(1)\text{--Cl}(1) = 2.2738(7)$ ,  $\text{Co}(1)\text{--Cl}(2) = 2.2713(7)$ ;  $\text{C}(1)\text{--Co}(1)\text{--C}(22) = 124.95(9)$ ,  $\text{Cl}(1)\text{--Co}(1)\text{--Cl}(2) = 103.21(3)$ ,  $\text{C}(1)\text{--Co}(1)\text{--Cl}(2) = 100.86(6)$ ,  $\text{C}(22)\text{--Co}(1)\text{--Cl}(1) = 98.89(6)$ .

ligands is identical with that observed in Fe(II) chemistry. Moreover, the solid-state structures of  $[\text{CoCl}_2(\text{IMes})_2]$  (vide infra) and  $[\text{Co}_2(\mu\text{-Cl})_2\text{Cl}_2(\text{IPr})_2]$  are very similar to those of the iron analogues, further demonstrating a close structural homology.

Crystallization of  $[\text{CoCl}_2(\text{IMes})_2]$  from benzene/pentane afforded crystals suitable for X-ray diffraction. The solid-state structure of the complex is depicted in Figure 1 (crystallographic data can be found in Table S1 of the SI). As with the iron analogue,  $[\text{CoCl}_2(\text{IMes})_2]$  displays a grossly distorted tetrahedral geometry about the Co(II) ion with a C–Co–C bond angle of  $124.95(9)^\circ$ . The average Co–C<sub>carbene</sub> bond length of 2.08  $\text{\AA}$  is similar to that reported for iron (average of 2.15  $\text{\AA}$ ), but with a slight contraction, as expected for the smaller covalent radius of Co(II). In sum, the bond metrics of  $[\text{CoCl}_2(\text{IMes})_2]$  are similar to those of the related Co(II) species  $[\text{CoCl}_2\{\text{PhB}(\text{MesIm})_2(\text{MesImH})\}]$  prepared by Smith, which contains a chelating carbene ligand.<sup>36</sup> However,  $[\text{CoCl}_2(\text{IMes})_2]$  demonstrates an overall expansion about the core metric parameters consistent with the greater steric bulk of the unconstrained IMes ligand.

To examine the possibility of the  $[\text{CoCl}_2(\text{IMes})_2]$  complex serving as a precursor to other reduced and oxidized Co complexes, we turned to cyclic voltammetry. We first explored the electrochemical behavior of the complex at higher potentials, reasoning that a reversible  $\text{Co}^{\text{II/III}}$  couple may be observed, as found for the iron system. This proved to be the case, with  $[\text{CoCl}_2(\text{IMes})_2]$  displaying a reversible  $\text{Co}^{\text{II/III}}$  couple in  $\text{CH}_2\text{Cl}_2$  at  $+0.310$  V vs  $\text{Fc}/\text{Fc}^+$  (see Figure S3 in the SI). Attempted chemical oxidation of this species with both  $\text{Ag}^+$  and  $\text{NO}^+$  salts did not produce the desired Co(III) species but rather led to apparent loss of one IMes ligand and formation of the dimeric chloro-bridged complex  $[\text{Co}_2(\mu\text{-Cl})_2\text{Cl}_2(\text{IMes})_2]$  (Scheme 2 and Figure S4, SI). These reactions did not proceed cleanly, or in high yield, and the nature of the carbene-containing byproduct was not established. The dimeric species could be prepared independently from  $\text{CoCl}_2$  and 1 equiv of IMes; however, difficulties with isolation of this species due to

its poor solubility in solvents other than THF led us to forego further investigation.

In contrast to the single well-behaved anodic event observed for  $[\text{CoCl}_2(\text{IMes})_2]$  at positive potentials, examination of the low-potential regime in THF revealed several irreversible processes (Figure 2). The first irreversible process occurs at

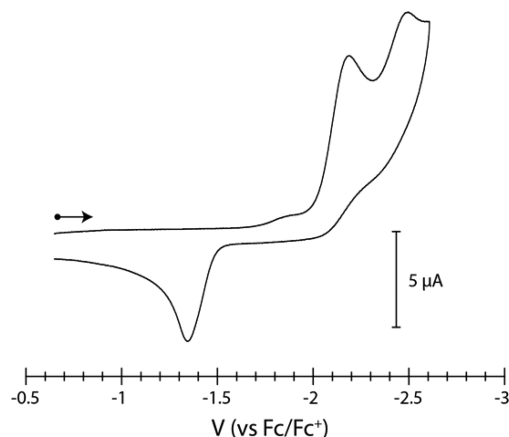


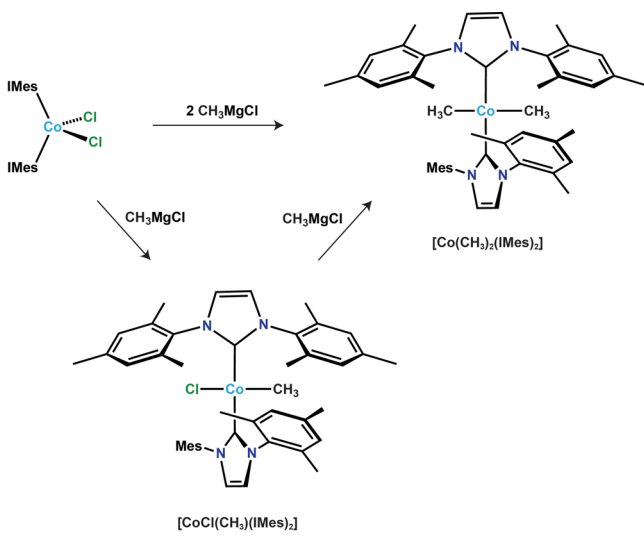
**Figure 2.** Cyclic voltammogram of  $[\text{CoCl}_2(\text{IMes})_2]$  (1 mM) at a glassy-carbon electrode in THF, showing the cathodic events observed at low potentials. The scan rate is 100 mV/s, and the supporting electrolyte is 0.2 M  $\text{Bu}_4\text{NPF}_6$ . See Figure S6 (SI) for the full voltammogram.

$-2.19$  V and may correspond to formation of the previously reported Co(I) species  $[\text{CoCl}(\text{IMes})_2]$  via subsequent loss of one chloride ligand.<sup>46</sup> A corresponding irreversible anodic process is observed at  $-1.34$  V in the return wave, which is not present unless the aforementioned irreversible cathode process takes place. These two events are reasonably stable through multiple scans, although some change in the peak currents is observed (Figure S5, SI). Further scanning to negative potentials in THF results in a second irreversible wave near  $-2.5$  V, which we cannot assign at this time but favor as a Co(0) species. In total, these results demonstrate that up to

four different oxidation states of the Co NHC may be accessible electrochemically if each event corresponds to a true metal-based redox process.

**Alkyl Complexes.** Alkylation of  $[\text{CoCl}_2(\text{IMes})_2]$  with 2 equiv of  $\text{CH}_3\text{MgCl}$  in THF afforded a canary yellow complex that we assign as *trans*- $[\text{Co}(\text{CH}_3)_2(\text{IMes})_2]$  (Scheme 3) on the

Scheme 3



basis of solution spectroscopic measurements and X-ray crystallography (vide infra). The NMR spectrum of the material in benzene- $d_6$  (see Figure S7 in the SI) displays four peaks for the IMes ligand, demonstrating the time-averaged  $D_{2h}$  symmetry expected for a square-planar geometry. The square-planar nature of this species is in line with that of  $[\text{Co}(\text{IMes}')_2]$  (Scheme 1) and also with that of the iron analogue recently described by Ohki, Tatsumi, Glorius, and co-workers.<sup>24</sup> Solution magnetic susceptibility measurements on  $[\text{Co}(\text{CH}_3)_2(\text{IMes})_2]$  give a magnetic moment of  $2.5(2) \mu_B$ , consistent with formulation of the complex as low-spin Co(II).<sup>45,48,49</sup> This assignment also agrees with that for the iron(II) analogue, which was described as intermediate spin ( $S = 1$ ).<sup>24</sup>

The solid-state structure of  $[\text{Co}(\text{CH}_3)_2(\text{IMes})_2]$  is shown in Figure 3. The structure contains two crystallographically independent molecules in the asymmetric unit, which each reside on a special position (see the SI). The geometry about Co is unequivocally square planar with bond angles of almost exactly  $90^\circ$ . The Co–C<sub>carbene</sub> bond length of 1.915(2) Å is notably shorter than that of  $[\text{CoCl}_2(\text{IMes})_2]$ , exhibiting the effect of changing from high-spin to low-spin Co(II). The average Co–C<sub>Me</sub> bond length of 2.04 Å is similar to those of other Co(II) methyl complexes in tetrahedral geometries<sup>36,50–52</sup> but longer than the distances reported for square-planar Co(II) methyl complexes containing chelating pyridine-based ligands.<sup>35,49,53,54</sup>

Cyclic voltammetry measurements of  $[\text{Co}(\text{CH}_3)_2(\text{IMes})_2]$  display several irreversible anodic processes in THF (Figure S8, SI). The first of these events occurs at  $-1.15$  V, demonstrating the reduced nature of this Co(II) species with respect to  $[\text{CoCl}_2(\text{IMes})_2]$ . No assignable cathodic events were detected within the solvent window, suggesting that formation of a singlet Co(I) dimethyl species is not readily feasible. Also consistent with this finding is the observation that  $[\text{Co}$

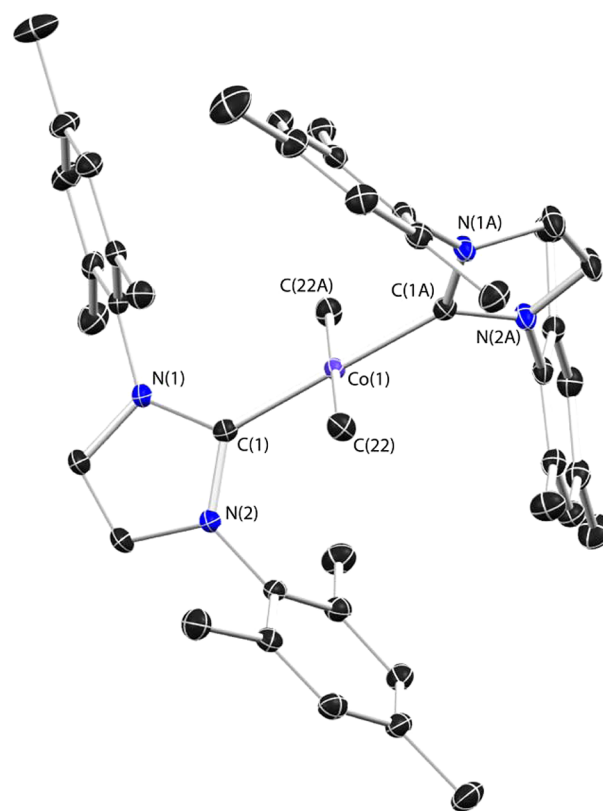
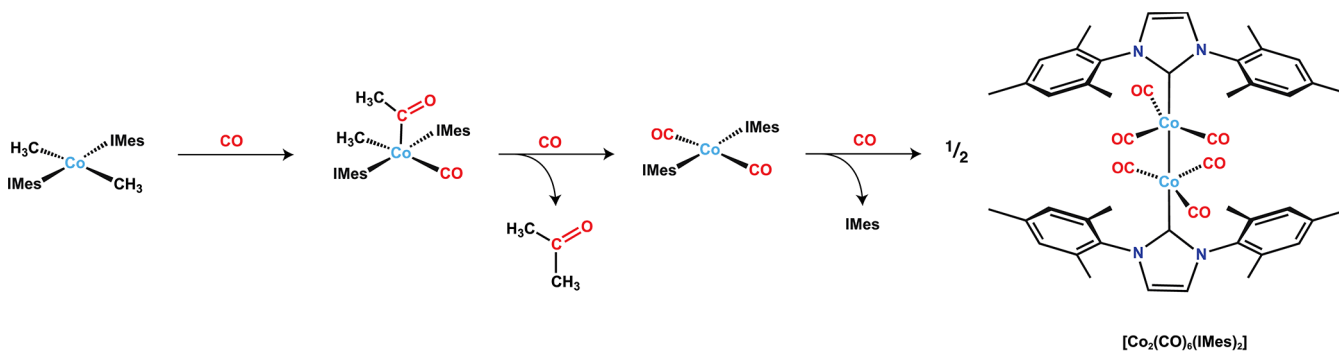


**Figure 3.** Thermal ellipsoid drawing (50%) of one of the independent molecules of  $[\text{Co}(\text{CH}_3)_2(\text{IMes})_2]$  in the asymmetric unit. Hydrogen atoms are omitted for clarity. Selected bond lengths (Å) and angles (deg): Co(1)–C(1) = 1.915(2), Co(1)–C(22) = 2.037(2); C(1)–Co(1)–C(1A) = 179.52(10), C(22)–Co(1)–C(22A) = 179.67(11), C(1)–Co(1)–C(22) = 90.65(7), C(1)–Co(1)–C(22A) = 89.35(7).

$(\text{CH}_3)_2(\text{IMes})_2]$  does not react with excess  $\text{PhMgCl}$  or  $\text{EtMgCl}$ .

NMR spectra of several preparations of  $[\text{Co}(\text{CH}_3)_2(\text{IMes})_2]$  revealed the presence of a second Co complex in small quantities prior to purification. The spectroscopic features of this unknown compound resemble those of  $[\text{Co}(\text{CH}_3)_2(\text{IMes})_2]$  but contain additional resonances consistent with lower overall symmetry (Figure S9, SI). Addition of excess  $\text{CH}_3\text{MgCl}$  to the unknown compound results in formation of  $[\text{Co}(\text{CH}_3)_2(\text{IMes})_2]$ . Together, these observations point to the identity of the unknown compound as the monomethyl complex  $[\text{CoCl}(\text{CH}_3)(\text{IMes})_2]$ . Such a compound is very intriguing, given that it represents a possible catalytic intermediate arising from oxidative addition of an alkyl halide to Co(0). Attempts to synthesize the compound in pure form through reaction of  $[\text{CoCl}_2(\text{IMes})_2]$  with 1 equiv of  $\text{CH}_3\text{MgCl}$  invariably resulted in small amounts of the dimethyl complex being formed in tandem; however, orange crystals of  $[\text{CoCl}(\text{CH}_3)(\text{IMes})_2]$  suitable for X-ray diffraction were obtained by vapor diffusion of pentane into a saturated benzene solution of the complex. The solid-state structure (Figure S10, SI) suffers from a positional disorder of the  $\text{CH}_3$  and Cl ligands and therefore could not be refined to a satisfactory degree. However, the structure does confirm the square-planar geometry of the complex and the shortened Co–C<sub>carbene</sub> bond distances, as observed in the dimethyl species. Thus, it appears that the geometry and spin-state change occur after addition of the first methyl group to  $[\text{CoCl}_2(\text{IMes})_2]$ .

Scheme 4



Efforts to synthesize mixed alkyls by reaction of  $[\text{CoCl}(\text{CH}_3)(\text{IMes})_2]$  with other Grignards were unsuccessful, leading to intractable products in the case of  $\text{EtMgCl}$  and no reaction in the case of  $\text{PhMgCl}$ .

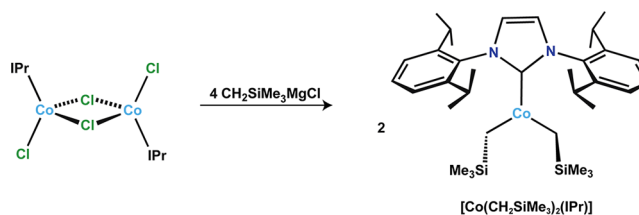
Attempts to prepare other dialkyl species of  $\text{IMes-Co(II)}$  using  $\text{EtMgCl}$  and  $\text{PhMgCl}$  resulted in a mixture of species, as judged by NMR spectroscopy. A major component of these mixtures was found to be the  $\text{Co(I)}$  species  $[\text{CoCl}(\text{IMes})_2]$ , on the basis of the appearance of resonances at  $-15.7$  and  $-21.7$  ppm.<sup>46</sup> Thus, reduction to  $\text{Co(I)}$  by these Grignard reagents appears to be a competing side reaction hindering formation of the desired  $\text{Co(II)}$  alkyls. Whether such reductions occur as a result of direct outer-sphere electron transfer or by subsequent decomposition of the putative alkyls remains to be determined. It should be noted, however, that no ethylene was detected during in situ alkylations of  $[\text{CoCl}_2(\text{IMes})_2]$  employing  $\text{EtMgCl}$ , arguing against  $\beta$ -hydrogen elimination as a major decomposition pathway. The formation of biphenyl, however, was detected in a number of catalytic reactions with  $[\text{CoCl}_2(\text{IMes})_2]$  and  $\text{PhMgCl}$  (vide infra). These alkylation results are consistent with those obtained for aryl-substituted NHCs of iron, where the only alkyl species prepared to date possess  $\text{Me}$ ,  $\text{benzyl}$ , or  $\text{CH}_2\text{SiMe}_3$  ligands.

The reactivity of  $[\text{Co}(\text{CH}_3)_2(\text{IMes})_2]$  with  $\text{CO}$  was examined to establish if such compounds display insertion chemistry<sup>52</sup> and to compare the resulting products with those obtained for  $[\text{Co}(\text{IMes}')_2]$ .<sup>46</sup> Treatment of a benzene- $d_6$  solution of  $[\text{Co}(\text{CH}_3)_2(\text{IMes})_2]$  with excess  $\text{CO}$  ( $\sim 1$  atm) led to an immediate darkening of the solution and formation of a new diamagnetic product, as judged by NMR spectroscopy (Figure S11, SI). In addition to the new diamagnetic product, the spectrum contains resonances for free  $\text{IMes}$  and for acetone. On the basis of these observations, we assign the new diamagnetic cobalt species as the  $\text{Co(0)}$  dimer  $[\text{Co}_2(\text{CO})_6(\text{IMes})_2]$ .<sup>31</sup> We propose formation of this species occurs through  $\text{CO}$  insertion into one of the  $\text{Co-CH}_3$  bonds of the dimethyl complex followed by reductive elimination of acetone and dimerization of the resulting  $\text{Co(0)}$  species, as shown in Scheme 4. This result is in contrast with that found by Deng for reaction of  $[\text{Co}(\text{IMes}')_2]$  with  $\text{CO}$ , where formation of the putative  $\text{Co(0)}$  intermediate was found to undergo rapid  $\text{C-H}$  activation.<sup>46</sup> Such an outcome is consistent with the chelated nature of  $[\text{Co}(\text{IMes}')_2]$  versus  $[\text{Co}(\text{CH}_3)_2(\text{IMes})_2]$ , which hinders dissociation from the metal. The dimeric carbonyl species  $[\text{Co}_2(\text{CO})_6(\text{IMes})_2]$  was not observed to be very stable, as judged by changes to its IR spectrum upon standing in solution (Figure S12, SI). Similar behavior was noted in previous reports of the molecule.<sup>31,55</sup> Attempted

crystallization from the reaction mixture described above afforded the cobaltate species  $(\text{IMes}\cdot\text{H}^+)[\text{Co}(\text{CO})_3(\text{IMes})]$  (Figure S13, SI), along with other unidentified paramagnetic  $\text{Co}$  species after several weeks.

Alkylation of dimeric  $[\text{Co}_2(\mu\text{-Cl})_2\text{Cl}_2(\text{IPr})_2]$  with 4 equiv of  $\text{Me}_3\text{SiCH}_2\text{MgCl}$  also afforded a yellow compound that we assign as the three-coordinate  $\text{Co(II)}$  complex  $[\text{Co}(\text{CH}_2\text{SiMe}_3)_2(\text{IPr})]$  (Scheme 5). Similar reactions with

Scheme 5



$\text{PhCH}_2\text{MgCl}$  yielded material consistent with the dibenzyl analogue, as judged by NMR spectroscopy; however, attempts to isolate the complex were unsuccessful. The NMR spectrum (Figure S14, SI) of  $[\text{Co}(\text{CH}_2\text{SiMe}_3)_2(\text{IPr})]$  is consistent with a paramagnetic  $\text{Co(II)}$  species displaying time-averaged  $\text{C}_{2v}$  symmetry in solution, as expected for a trigonal-planar species. Unlike the dimethyl complex, solution magnetic susceptibility measurements provided a much larger value for the magnetic moment of  $5.1(2) \mu_{\text{B}}$ , pointing to a monomeric high-spin  $\text{Co(II)}$  center displaying a significant orbital contribution. Such contributions to the magnetic moment were also observed for the three-coordinate iron analogue<sup>23</sup> as well as other three-coordinate  $\text{Co(II)}$  complexes bearing  $\beta$ -diketiminato ligands.<sup>56</sup>

The solid-state structure of  $[\text{Co}(\text{CH}_2\text{SiMe}_3)_2(\text{IPr})]$  is depicted in Figure 4. The structure is analogous to that of the iron analogue, displaying a trigonal-planar geometry about  $\text{Co}$  with the imidazolylidene group of the  $\text{IPr}$  ligand lying approximately within the  $\text{CoC}_3$  plane. Interestingly, comparison of the bond distances with those of  $[\text{Co}(\text{CH}_3)_2(\text{IMes})_2]$  reveals substantial elongation of the  $\text{Co-C}_{\text{carbene}}$  bond ( $2.097(3)$  vs  $1.915(2)$  Å). Consideration of the bond distances for the alkyl ligands reveals a less dramatic difference from that of the methyl complex ( $2.099(2)$  vs  $2.037(2)$  Å), but one that still highlights the important role of the spin state in these  $\text{Co(II)}$  alkyl complexes. Moreover, introduction of  $\text{CO}$  to benzene solutions of  $[\text{Co}(\text{CH}_2\text{SiMe}_3)_2(\text{IPr})]$  resulted in no reaction after 15–30 min, in contrast to the rapid reaction observed with  $[\text{Co}(\text{CH}_3)_2(\text{IMes})_2]$ , suggesting that  $\text{CO}$  reactivity occurs much more readily with the low-spin species.<sup>57</sup> After an extended time (36 h), the reaction of  $[\text{Co}(\text{CH}_2\text{SiMe}_3)_2(\text{IPr})]$

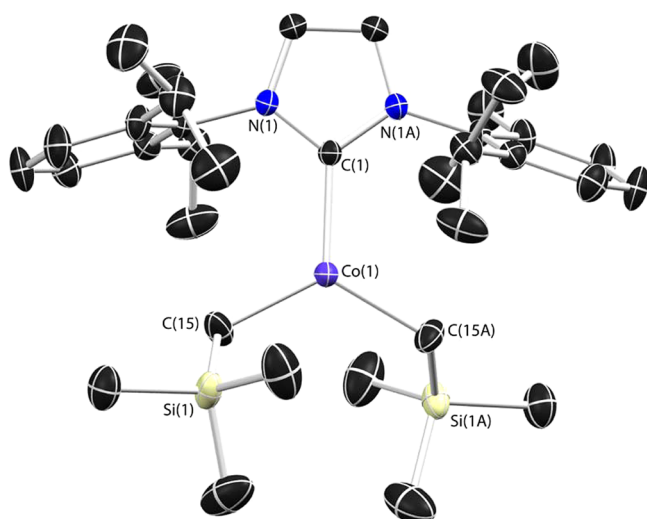


**Figure 4.** Thermal ellipsoid drawing (50%) of  $[\text{Co}_2(\text{CH}_2\text{SiMe}_3)_2(\text{IPr})]$ . Hydrogen atoms and the minor component of one disordered  $^i\text{Pr}$  group are omitted for clarity. Selected bond lengths (Å) and angles (deg):  $\text{Co}(1)\text{--C}(1) = 2.097(3)$ ,  $\text{Co}(1)\text{--C}(15) = 2.099(2)$ ;  $\text{C}(1)\text{--Co}(1)\text{--C}(15) = 118.67(8)$ ,  $\text{C}(15)\text{--Co}(1)\text{--C}(15A) = 122.66(16)$ .

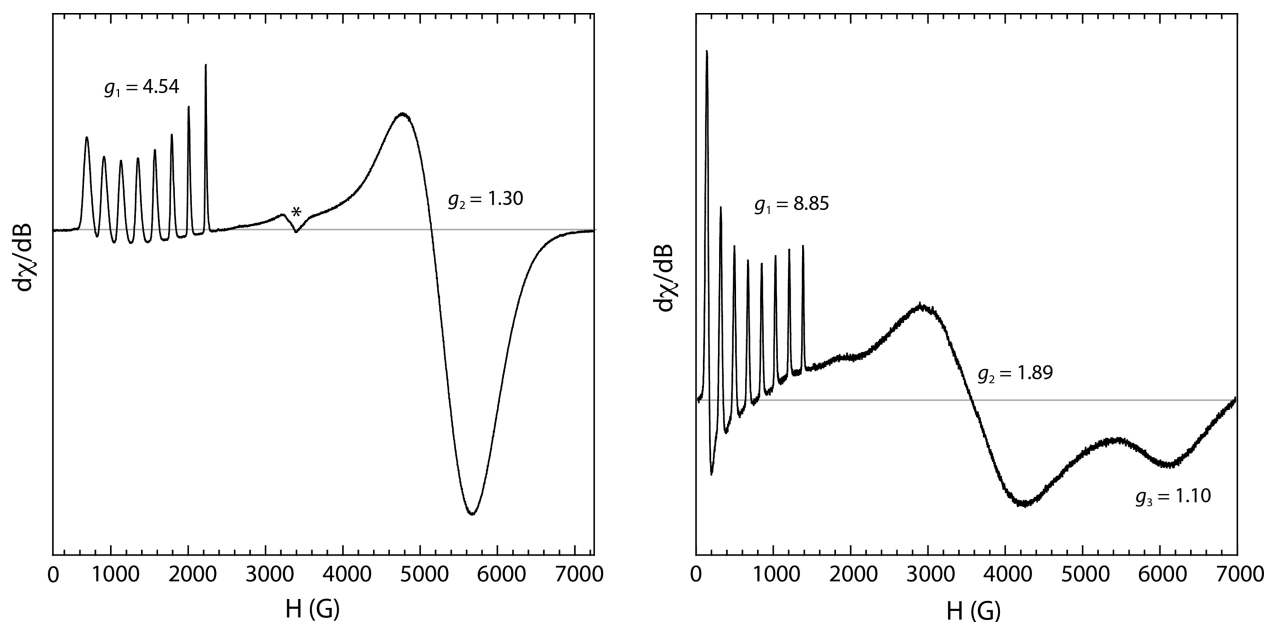
and CO was found to yield a purple solution. The nature of this purple solution has not been determined at this time; however, IR spectra display a peak at  $1700\text{ cm}^{-1}$  consistent with formation of organic carbonyl species.

Cyclic voltammetry measurements on  $[\text{Co}(\text{CH}_2\text{SiMe}_3)_2(\text{IPr})]$  also yielded results markedly different from those of the dimethyl complex. Unlike  $[\text{Co}(\text{CH}_3)_2(\text{IMes})_2]$ , the CV of  $[\text{Co}(\text{CH}_2\text{SiMe}_3)_2(\text{IPr})]$  in THF displays several irreversible reduction events more comparable to those observed with  $[\text{CoCl}_2(\text{IMes})_2]$ , but at lower potentials (Figure S15, SI). These events change upon repeated cycling of the potential, suggesting that initial reduction of the complex leads to further chemistry. The possibility for reduction of

$[\text{Co}(\text{CH}_2\text{SiMe}_3)_2(\text{IPr})]$  is also consistent with stoichiometric reactions carried out with Grignard reagents.  $[\text{Co}(\text{CH}_2\text{SiMe}_3)_2(\text{IPr})]$  reacts readily with both  $\text{EtMgCl}$  and  $\text{PhMgCl}$  to afford mixtures of paramagnetic species, as judged by  $^1\text{H}$  NMR spectroscopy.

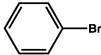
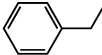
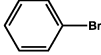
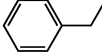
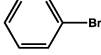
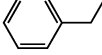
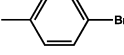
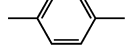
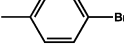
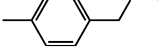
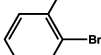
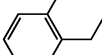
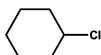
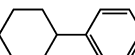
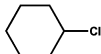
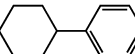
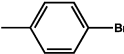
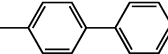
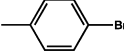
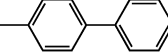
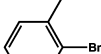
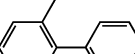
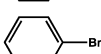
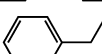
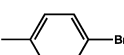
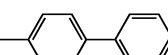
**EPR Spectroscopy.** To examine the electronic nature of the two dialkyl species, preliminary EPR studies were undertaken. The spectra of both  $[\text{Co}(\text{CH}_3)_2(\text{IMes})_2]$  and  $[\text{Co}(\text{CH}_2\text{SiMe}_3)_2(\text{IPr})]$  were recorded at 4.2 K in a 2-MeTHF glass and appear in Figure 5. The spectrum of  $[\text{Co}(\text{CH}_3)_2(\text{IMes})_2]$  displays an axial signal, as expected for the square-planar geometry of the complex. Hyperfine coupling to  $^{59}\text{Co}$  is well-resolved in the  $g_{\parallel}$  component ( $A_{\text{Co}} = 223\text{ G}$ ), suggesting that the unpaired electron resides in an orbital of predominantly  $d_{z^2}$  character. This assignment agrees with that for the homoleptic Co(II) carbene  $[\text{Co}(\text{IEt})_4](\text{BF}_4)_2$  prepared by Deng;<sup>45</sup> however, the  $g$  values observed for  $[\text{Co}(\text{CH}_3)_2(\text{IMes})_2]$  are outside the range typically encountered for low-spin Co(II).<sup>49,58</sup> The EPR spectrum of trigonal-planar  $[\text{Co}(\text{CH}_2\text{SiMe}_3)_2(\text{IPr})]$  displays a rhombic signal with  $g$  values of 8.85, 1.89, and 1.10, consistent with a quartet ground state. Well-resolved hyperfine coupling to the  $^{59}\text{Co}$  is observed for the  $g_1$  component ( $A_{\text{Co}} = 177\text{ G}$ ).

**Catalytic Trials.** To determine the catalytic efficacy of the cobalt complexes in C–C coupling reactions, several Kumada-type couplings were investigated employing  $[\text{CoCl}_2(\text{IMes})_2]$  as a precatalyst. Three different combinations of coupling partners, alkyl–aryl, aryl–alkyl, and aryl–aryl, were examined as displayed in Table 1. The results of the catalytic trials are consistent with those reported for  $[\text{Co}_2(\mu\text{-Cl})_2\text{Cl}_2(\text{IPr})_2]$ ,<sup>47</sup> in that aryl–aryl couplings catalyzed by  $[\text{CoCl}_2(\text{IMes})_2]$  appear to be the most successful, leading to complete or nearly complete conversions (entries 9–11). Substantially less conversion was observed for couplings between alkyl Grignards and aryl electrophiles, and essentially no conversion was observed for couplings employing  $\text{PhMgCl}$  and chlorocyclohexane (aryl–alkyl). Performing reactions at elevated ( $50\text{ }^\circ\text{C}$ ) and reduced



**Figure 5.** X-band EPR spectra of  $[\text{Co}(\text{CH}_3)_2(\text{IMes})_2]$  (left) and  $[\text{Co}(\text{CH}_2\text{SiMe}_3)_2(\text{IPr})]$  (right) in 2-MeTHF glasses at 4.2 K. The asterisk denotes an impurity from the EPR cavity.

Table 1. Results from Kumada Coupling Reactions Employing  $[\text{CoCl}_2(\text{IMes})_2]^a$ 

Entry	Temperature (°C)	Nucleophile	Electrophile	Product	% Conversion <sup>b</sup>
1	25	EtMgCl			28
2	50	EtMgCl			21
3	-20	EtMgCl			9.5
4	25	MeMgCl			21
5	25	$\text{Me}_3\text{SiCH}_2\text{MgCl}$			13
6	-20	EtMgCl			14
7	25	PhMgCl			< 2 (10)
8	-20	PhMgCl			< 2 (11)
9	25	PhMgCl			> 98 (10)
10	-20	PhMgCl			81 (15)
11	25	PhMgCl			61 (5) <sup>d</sup>
12 <sup>c</sup>	25	EtMgCl			32
13 <sup>c</sup>	25	PhMgCl			> 98 (9)

<sup>a</sup>Reactions performed in THF with 2 mol % catalyst loading. <sup>b</sup>Determined by GC-MS with respect to electrophile. Values in parentheses denote the amount of biphenyl formed. <sup>c</sup>Reactions performed in THF with 2 mol %  $[\text{Co}(\text{CH}_2\text{SiMe}_3)_2(\text{IPr})]$  as precatalyst. <sup>d</sup>4% 2,2'-dimethylbiphenyl also detected.

temperatures (-20 °C) resulted in similar to lower conversions for selected couplings. Aryl electrophiles therefore appear to be the most successful coupling partners in reactions employing Co(II) NHCs.<sup>19</sup> In all reactions employing PhMgCl, ca. 10% of biphenyl was detected, signaling that reduction of Co(II) is most likely an important initiation step. Such a conclusion is consistent with stoichiometric reactions employing PhMgCl (vide supra) and argues for the role of lower valent cobalt species in mediating C–C coupling reactions. Interestingly, catalytic trials employing MeMgCl and  $\text{Me}_3\text{SiCH}_2\text{MgCl}$  (entries 4 and 5) also yielded the expected coupling products with conversions similar to that observed for EtMgCl. The reactivity of  $\text{Me}_3\text{SiCH}_2\text{MgCl}$  is unsurprising, given results with  $[\text{Co}(\text{CH}_2\text{SiMe}_3)_2(\text{IPr})]$  (vide infra). The results with MeMgCl, however, demonstrate that species other than  $[\text{Co}(\text{CH}_3)_2(\text{IMes})_2]$  are most likely generated under the catalytic conditions, since the dimethyl complex displays no stoichiometric reactivity with MeMgCl or bromobenzene, as judged by <sup>1</sup>H NMR spectroscopy.

Employing  $[\text{Co}(\text{CH}_3)_2(\text{IMes})_2]$  as a precatalyst resulted in no conversion to 4-methylbiphenyl in reactions of PhMgCl with 4-bromotoluene. However, small amounts (<15%) of ethylbenzene were observed in catalytic trials employing

EtMgCl and bromobenzene. Since  $[\text{Co}(\text{CH}_3)_2(\text{IMes})_2]$  does not react with either excess EtMgCl or bromobenzene, we attribute the observed activity to small quantities (<2%) of  $[\text{CoCl}(\text{CH}_3)(\text{IMes})_2]$  present in samples of the dimethyl complex. As noted,  $[\text{CoCl}(\text{CH}_3)(\text{IMes})_2]$  reacts rapidly with EtMgCl, whereas  $[\text{Co}(\text{CH}_3)_2(\text{IMes})_2]$  does not. Thus, the monomethyl species appears chemically competent in catalytic reactions employing alkyl Grignard reagents. The formation of the monomethyl complex during catalytic reactions employing MeMgCl may also explain the appearance of coupled products when  $[\text{CoCl}_2(\text{IMes})_2]$  is used as the precatalyst (entry 4).

In contrast to the dimethyl species,  $[\text{Co}(\text{CH}_2\text{SiMe}_3)_2(\text{IPr})]$  proved to be active for both aryl–aryl and alkyl–aryl couplings, resulting in conversions nearly identical with those obtained when  $[\text{CoCl}_2(\text{IMes})_2]$  was used as the precatalyst (entries 12 and 13). We propose that reduction of  $[\text{Co}(\text{CH}_2\text{SiMe}_3)_2(\text{IPr})]$  by the Grignard is a likely activation step that does not take place with  $[\text{Co}(\text{CH}_3)_2(\text{IMes})_2]$ . This proposal is consistent with the stoichiometric reactivity observed for each dialkyl complex in the presence of Grignard reagents and further highlights the importance of coordination number and spin state in these Co(II) complexes.  $[\text{Co}(\text{CH}_2\text{SiMe}_3)_2(\text{IPr})]$  was also found to react with bromobenzene to afford unidentified

paramagnetic species, albeit on a time scale much slower than that of the catalytic reactions.

## CONCLUSIONS

Several aryl-substituted NHC complexes of Co(II) have been prepared and characterized in solution and the solid state. Chloro complexes of Co(II) exist as high-spin species, displaying pseudotetrahedral geometries about the metal center. Alkylation of the IMes complex  $[\text{CoCl}_2(\text{IMes})_2]$  with 1 or 2 equiv of  $\text{MeMgCl}$  affords low-spin, square-planar Co(II) methyl complexes containing one or two  $\text{CH}_3$  ligands, respectively. The monomethyl species  $[\text{CoCl}(\text{CH}_3)(\text{IMes})_2]$  demonstrates reactivity with select alkyl Grignard reagents, providing a possible pathway for its involvement in C–C cross-coupling reactions. In contrast, the dimethyl species  $[\text{Co}(\text{CH}_3)_2(\text{IMes})_2]$  is inert toward Grignard reagents and aryl electrophiles, arguing against its direct involvement in such processes. Furthermore, catalytic reactions initiated with  $[\text{Co}(\text{CH}_3)_2(\text{IMes})_2]$  do not afford substantial quantities of the expected coupling products.  $[\text{Co}(\text{CH}_3)_2(\text{IMes})_2]$  does react with CO, resulting in formation of carbonyl complexes of reduced Co. Alkylation of the IPr complex  $[\text{Co}_2(\mu\text{-Cl})_2\text{Cl}_2(\text{IPr})_2]$  with  $\text{Me}_3\text{SiCH}_2\text{MgCl}$  produces three-coordinate, high-spin  $[\text{Co}(\text{CH}_2\text{SiMe}_3)_2(\text{IPr})]$ . Unlike  $[\text{Co}(\text{CH}_3)_2(\text{IMes})_2]$ ,  $[\text{Co}(\text{CH}_2\text{SiMe}_3)_2(\text{IPr})]$  reacts readily with Grignard reagents but not CO and is an effective precatalyst for several cross-coupling reactions. Thus, high-spin three-coordinate dialkyl species such as  $[\text{Co}(\text{CH}_2\text{SiMe}_3)_2(\text{IPr})]$  may resemble intermediates in C–C cross-coupling reactions catalyzed by Co(II) salts. Finally, the structures of all Co(II) species determined in the present work are very similar to those reported for iron(II), demonstrating a close similarity in their structural chemistry.

## EXPERIMENTAL SECTION

**General Comments.** All manipulations were performed under an atmosphere of nitrogen gas using standard Schlenk techniques or in a Vacuum Atmospheres glovebox under an atmosphere of purified nitrogen. Tetrahydrofuran, diethyl ether, methylene chloride, pentane, and toluene were purified by sparging with argon and passage through two columns packed with 4 Å molecular sieves. Benzene, benzene- $d_6$ , and 2-methyltetrahydrofuran were dried over sodium and then vacuum-distilled. All solvents were stored in the glovebox over 4 Å molecular sieves prior to use.  $^1\text{H}$  NMR spectra were recorded in benzene- $d_6$  on a Varian INOVA spectrometer operating at 500 MHz and referenced to the residual  $\text{C}_6\text{D}_5\text{H}$  peak of the solvent ( $\delta$  7.16 ppm vs TMS). UV–vis spectra were recorded at ambient temperature on a Cary-60 spectrophotometer in airtight Teflon-capped quartz cells. Cyclic voltammetry measurements were performed in a single-compartment cell under a nitrogen atmosphere at 23 °C using a CH Instruments 620D electrochemical workstation. A three-electrode setup was employed comprising a glassy-carbon working electrode, platinum-wire auxiliary electrode, and Ag/AgCl quasi-reference electrode. Triply recrystallized  $\text{Bu}_4\text{NPF}_6$  was used as the supporting electrolyte. All electrochemical data were referenced internally to the ferrocene/ferrocenium couple at 0.00 V. EPR measurements were recorded in 4 mm quartz tubes on a Bruker E500 EPR spectrometer operating at the X-band at a modulation frequency of 100 kHz and modulation amplitude of 10 G. Low-temperature measurements were made in frozen 2-MeTHF glasses at 4.2 K with temperature control maintained by a helium flow cryostat (ESR900, Oxford Instruments, Inc.). Solution magnetic susceptibility measurements were determined by the Evans method in benzene- $d_6$  without a solvent correction using reported diamagnetic corrections.<sup>59</sup> Elemental analyses were performed by Midwest Microlab, LLC, in Indianapolis, IN.

**Materials.** Carbene ligands IMes and IPr were prepared according to the literature procedure.<sup>60</sup> Anhydrous  $\text{CoCl}_2$  was purchased from Strem Chemical Co. and used as received. All other reagents were purchased from commercial vendors and used as received.

### X-ray Data Collection and Structure Solution Refinement.

Crystals suitable for X-ray diffraction were mounted in Paratone oil onto a glass fiber and frozen under a nitrogen cold stream. The data were collected at 98(2) K using a Rigaku AFC12/Saturn 724 CCD fitted with Mo  $K\alpha$  radiation ( $\lambda = 0.71073$  Å). Data collection and unit cell refinement were performed using Crystal Clear software.<sup>61</sup> Data processing and absorption correction, giving minimum and maximum transmission factors, were accomplished with Crystal Clear and ABCOR,<sup>62</sup> respectively. All structures were solved by direct methods and refined on  $F^2$  using full-matrix least-squares techniques with SHELXL-97.<sup>63,64</sup> All non-hydrogen atoms were refined with anisotropic displacement parameters. All carbon-bound hydrogen atom positions were determined by geometry and refined by a riding model. The structure of  $[\text{CoCl}(\text{CH}_3)(\text{IMes})_2]$  was found to be disordered about the Cl and  $\text{CH}_3$  groups. This disorder could not be refined satisfactorily, resulting in a structure from which only the geometry and connectivity of the atoms could be confidently determined (see Figure S10 in the SI).

**$[\text{CoCl}_2(\text{IMes})_2]$ .** A round-bottom flask was charged with 126 mg (975  $\mu\text{mol}$ ) of anhydrous  $\text{CoCl}_2$  and a solution of 592 mg (1.95 mmol) of IMes in 25 mL of THF. Once all solids had dissolved, the resulting blue solution was stirred for 16 h at ambient temperature. All volatiles were removed in vacuo, and the remaining blue residue was dissolved in a minimal amount of hot toluene. The saturated solution was chilled to  $-30$  °C for 4 h, during which time 595 mg (83% yield) of a blue solid precipitated. The solid material was isolated on a glass frit, washed with pentane, and dried in vacuo. Crystals suitable for X-ray diffraction were grown by vapor diffusion of pentane into a saturated benzene solution at 23 °C. The  $^1\text{H}$  NMR spectrum of the material at 20 °C is very broad; values at 75 °C are reported:  $\delta$  33.6 (br s, 4 =CH), 1.52 (s, 8 *m*-H), 1.01 (br s, 24 *o*-Me),  $-0.75$  (s, 12 *p*-Me).  $\mu_{\text{eff}} = 3.9(1)$   $\mu_{\text{B}}$ . UV–vis (toluene;  $\lambda$ , nm ( $\epsilon$ ,  $\text{M}^{-1} \text{cm}^{-1}$ )): 613 (sh), 639 (370), 664 (380). Anal. Calcd for  $\text{C}_{42}\text{H}_{48}\text{Cl}_2\text{CoN}_4$ : C, 68.29; H, 6.55; N, 7.58. Found: C, 67.78; H, 6.44; N, 7.77.

**$[\text{CoCl}_2(\mu\text{-Cl})_2(\text{IPr})_2]$ .** This molecule was prepared by reaction of 1 equiv of IPr with  $\text{CoCl}_2$  in THF as recently described.<sup>47</sup> UV–vis, X-ray crystallography, and solution magnetic susceptibility measurements were consistent with those of the reported compound. Since no NMR data were provided in the reported synthesis, we provide the chemical shifts here.  $^1\text{H}$  NMR:  $\delta$  37.05 (s, 4 =CH), 16.4 (br s, 8 *CHMe}\_2*), 4.53 (s, 24 *CHMe}\_2*),  $-0.06$  (s, 8 *m*-H),  $-0.71$  (s, 4 *p*-H),  $-1.40$  (s, 24 *CHMe}\_2*).  $\mu_{\text{eff}} = 5.2(1)$   $\mu_{\text{B}}$ . UV–vis (toluene;  $\lambda$ , nm ( $\epsilon$ ,  $\text{M}^{-1} \text{cm}^{-1}$ )): 570 (400), 656 (1400), 699 (1100).

**$[\text{CoCl}(\text{CH}_3)(\text{IMes})_2]$ .** A flask was charged with 270 mg (366  $\mu\text{mol}$ ) of  $[\text{CoCl}_2(\text{IMes})_2]$  and 10 mL of diethyl ether. The contents were stirred briefly to suspend the solids before the mixture was frozen at 77 K. To the thawing blue suspension was added 110  $\mu\text{L}$  (366  $\mu\text{mol}$ ) of 3.3 M  $\text{CH}_3\text{MgCl}$ . The mixture was stirred for 45 min, during which time it became green and then yellow. A precipitate persisted throughout the reaction time. All volatiles were removed in vacuo, and the remaining residue was dissolved in warm benzene, filtered through a glass frit, and then frozen. The frozen benzene was sublimed in vacuo to give 125 mg (49% yield) of an orange-yellow solid. Recrystallization of the solid from benzene/pentane afforded orange crystals. NMR spectra of recrystallized material repeatedly showed traces (5–15%) of the dimethyl complex. As a result, satisfactory elemental analyses were not obtained.  $^1\text{H}$  NMR:  $\delta$  76.0 (v br s, 3  $\text{CH}_3$ ), 44.7 (br s, 4 =CH),  $-3.61$  (br s, 12 *o*-Me),  $-5.47$  (br s, 12 *o*-Me),  $-6.37$  (s, 12 *p*-Me),  $-6.79$  (s, *m*-H),  $-7.69$  (s, *m*-H).

**$[\text{Co}(\text{CH}_3)_2(\text{IMes})_2]$ .** A flask was charged with 157 mg (213  $\mu\text{mol}$ ) of  $[\text{CoCl}_2(\text{IMes})_2]$  and 30 mL of THF. The blue solution was stirred briefly until homogeneous and then frozen at 77 K. To the thawing solution was added 140  $\mu\text{L}$  (446  $\mu\text{mol}$ ) of 3.3 M  $\text{CH}_3\text{MgCl}$ . The solution immediately turned green and was warmed to ambient temperature with stirring over 2.5 h. During this time the solution became yellow. All volatiles were removed in vacuo, and the remaining



residue was dissolved in a minimal amount of warm toluene and the solution filtered through Celite. The toluene was removed in vacuo to afford 101 mg (68% yield) of a yellow solid, which was washed with diethyl ether and dried in vacuo. Crystals suitable for X-ray diffraction were grown by vapor diffusion of pentane into a saturated benzene solution at 23 °C. <sup>1</sup>H NMR: δ 78.3 (v br, 6 CH<sub>3</sub>), 41.2 (br s, 4 =CH), -5.00 (br s, 24 *o*-Me), -5.87 (s, 12 *p*-Me), -6.02 (s, 8 *m*-H). μ<sub>eff</sub> = 2.4(1) μ<sub>B</sub>. UV-vis (toluene; λ, nm (ε, M<sup>-1</sup> cm<sup>-1</sup>)): 378 (2720). Repeated analyses consistently yielded low values for C, as has been observed in other NHC systems.<sup>21</sup> Anal. Calcd for C<sub>44</sub>H<sub>54</sub>CoN<sub>4</sub>: C, 75.73; H, 7.80; N, 8.03. Found: C, 74.51; H, 7.52; N, 7.93.

**[Co(CH<sub>2</sub>SiMe<sub>3</sub>)<sub>2</sub>(IPr)].** A flask was charged with 188 mg (182 μmol) of [Co<sub>2</sub>Cl<sub>2</sub>(μ-Cl)<sub>2</sub>(IPr)<sub>2</sub>] and 25 mL of diethyl ether. The resulting blue suspension was briefly stirred and then chilled to -30 °C. To the chilled suspension was added 1.0 mL (1.0 mmol) of 1.0 M Me<sub>3</sub>SiCH<sub>2</sub>MgCl. The suspension quickly became yellow and was allowed to react for 5 min with warming to ambient temperature. All volatiles were then removed in vacuo, and the resulting yellow residue was extracted into pentane and the extract filtered through glass filter paper. Evaporation of the pentane afforded 203 mg (89% yield) of a yellow solid. Crystals suitable for X-ray diffraction were grown by slow cooling of a saturated pentane solution at -30 °C. <sup>1</sup>H NMR: δ 27.9 (br s, 4 CHMe<sub>2</sub>), 27.11 (s, 18 SiMe<sub>3</sub>), 12.94 (s, 12 CHMe<sub>2</sub>), -22.09 (s, 2 *p*-H), -26.05 (s, 4 *m*-H), -70.04 (s, 12 CHMe<sub>2</sub>), -101.85 (s, 2 =CH). μ<sub>eff</sub> = 5.1(1) μ<sub>B</sub>. UV-vis (toluene; λ, nm (ε, M<sup>-1</sup> cm<sup>-1</sup>)): 313 (3020). Anal. Calcd for C<sub>33</sub>H<sub>58</sub>CoN<sub>2</sub>Si<sub>2</sub>: C, 67.93; H, 9.45; N, 4.53. Found: C, 67.33; H, 9.18; N, 4.54.

**Reaction of [Co(CH<sub>3</sub>)<sub>2</sub>(IMes)<sub>2</sub>] with CO To Form [Co<sub>2</sub>(CO)<sub>6</sub>(IMes)<sub>2</sub>].** A ~20 mM solution of [Co(CH<sub>3</sub>)<sub>2</sub>(IMes)<sub>2</sub>] in benzene-*d*<sub>6</sub> was transferred to an NMR tube that was sealed with a septum. An excess of CO gas was introduced to the headspace of the tube via a needle through the septum cap. The solution immediately darkened, and NMR and IR spectra were recorded within 15 min. See Figures S11 and S12 (SI) for spectra. Protracted standing of the reaction solution at ambient temperature resulted in IR spectra different from those obtained immediately after the introduction of CO (Figure S12, SI). Subjection of the reaction mixture to vapor diffusion of pentane afforded crystals of the cobaltate species (IMes-H)[Co(CO)<sub>3</sub>(IMes)] after 2 weeks (Figure S13, SI). <sup>1</sup>H NMR for [Co<sub>2</sub>(CO)<sub>6</sub>(IMes)<sub>2</sub>] immediately after reaction: δ 6.76 (s, 8 *m*-H), 6.09 (s, 4 =CH), 2.09 (s, 12 *p*-Me), 2.06 (s, 24 *o*-Me). IR (C<sub>6</sub>D<sub>6</sub> solution; cm<sup>-1</sup>): 2009 (ν<sub>CO</sub>), 1963 (ν<sub>CO</sub>), 1940 (ν<sub>CO</sub>).

**General Procedure for Catalytic Reactions Employing [CoCl<sub>2</sub>(IMes)<sub>2</sub>].** In a representative procedure, a scintillation vial was charged with 5.0 mg (6.8 μmol, 2 mol %) of [CoCl<sub>2</sub>(IMes)<sub>2</sub>] and 5 mL of THF. To the vial was added 339 μmol of the desired electrophile. The solution was stirred briefly before 339 μmol of the Grignard reagent was added in one portion. The reaction was stirred at ambient temperature for 1 h, after which time it was quenched with 5 mL of 2 M aqueous oxalic acid. The organic layer was separated using diethyl ether and an aliquot subjected to GC-MS analysis. All trials were repeated multiple times, and the products were confirmed by their MS signatures. Catalytic trials requiring low temperatures were carried out in a similar fashion at -20 °C by use of a dry ice/ethylene glycol bath. GC-MS analysis of control reactions carried out with both coupling partners in the presence of IMes or IPr did not produce a detectable amount of the coupled products or biphenyl.

## ■ ASSOCIATED CONTENT

### ■ Supporting Information

Figures S1–S15, Table S1, and CIF files containing additional structures, spectra, and crystallographic data. This material is available free of charge via the Internet at <http://pubs.acs.org>.

## ■ AUTHOR INFORMATION

### Corresponding Author

\*E-mail: zachary.tonzetich@utsa.edu.

## Notes

The authors declare no competing financial interest.

## ■ ACKNOWLEDGMENTS

This work was supported by startup funding from the University of Texas at San Antonio and by a grant from the Welch Foundation (AX-1772 to Z.J.T.). We thank Mr. Jonathan Caranto for assistance with EPR measurements.

## ■ REFERENCES

- (1) Díez-González, S.; Marion, N.; Nolan, S. P. *Chem. Rev.* **2009**, *109*, 3612–3676.
- (2) Hu, X.; Meyer, K. J. *Organomet. Chem.* **2005**, *690*, 5474–5484.
- (3) Tye, J. W.; Lee, J.; Wang, H.-W.; Mejia-Rodriguez, R.; Reibenspies, J. H.; Hall, M. B.; Darensbourg, M. Y. *Inorg. Chem.* **2005**, *44*, 5550–5552.
- (4) Capon, J.-F.; El Hassnaoui, S.; Gloaguen, F.; Schollhammer, P.; Talarmin, J. *Organometallics* **2005**, *24*, 2020–2022.
- (5) Morvan, D.; Capon, J.-F.; Gloaguen, F.; Le, G. A.; Marchivie, M.; Michaud, F.; Schollhammer, P.; Talarmin, J.; Yaouanc, J.-J.; Pichon, R.; Kervarec, N. *Organometallics* **2007**, *26*, 2042–2052.
- (6) Hess, J. L.; Hsieh, C.-H.; Reibenspies, J. H.; Darensbourg, M. Y. *Inorg. Chem.* **2011**, *50*, 8541–8552.
- (7) Ingleson, M. J.; Layfield, R. A. *Chem. Commun.* **2012**, *48*, 3579–3589.
- (8) Silberstein, A. L.; Ramgren, S. D.; Garg, N. K. *Org. Lett.* **2012**, *14*, 3796–3799.
- (9) Ghorai, S. K.; Jin, M.; Hatakeyama, T.; Nakamura, M. *Org. Lett.* **2012**, *14*, 1066–1069.
- (10) Xiang, L.; Xiao, J.; Deng, L. *Organometallics* **2011**, *30*, 2018–2025.
- (11) Gao, H.-H.; Yan, C.-H.; Tao, X.-P.; Xia, Y.; Sun, H.-M.; Shen, Q.; Zhang, Y. *Organometallics* **2010**, *29*, 4189–4192.
- (12) Li, B.-J.; Xu, L.; Wu, Z.-H.; Guan, B.-T.; Sun, C.-L.; Wang, B.-Q.; Shi, Z.-J. *J. Am. Chem. Soc.* **2009**, *131*, 14656–14657.
- (13) Danopoulos, A. A.; Pugh, D.; Smith, H.; Saßmannshausen, J. *Chem. Eur. J.* **2009**, *15*, 5491–5502.
- (14) Gosmini, C.; Begouin, J. M.; Moncomble, A. *Chem. Commun.* **2008**, 3221–3233.
- (15) Cahiez, G.; Moyeux, A. *Chem. Rev.* **2010**, *110*, 1435–1462.
- (16) Song, W.; Ackermann, L. *Angew. Chem., Int. Ed.* **2012**, *51*, 8251–8254.
- (17) Gao, K.; Yoshikai, N. *Chem. Commun.* **2012**, *48*, 4305–4307.
- (18) Gao, K.; Lee, P.-S.; Long, C.; Yoshikai, N. *Org. Lett.* **2012**, *14*, 4234–4237.
- (19) Hatakeyama, T.; Hashimoto, S.; Ishizuka, K.; Nakamura, M. *J. Am. Chem. Soc.* **2009**, *131*, 11949–11963.
- (20) Someya, H.; Ohmiya, H.; Yorimitsu, H.; Oshima, K. *Org. Lett.* **2007**, *9*, 1565–1567.
- (21) Przyojski, J. A.; Arman, H. D.; Tonzetich, Z. J. *Organometallics* **2012**, *31*, 3264–3271.
- (22) Danopoulos, A. A.; Braunstein, P.; Stylianides, N.; Wesolek, M. *Organometallics* **2011**, *30*, 6514–6517.
- (23) Danopoulos, A. A.; Braunstein, P.; Wesolek, M.; Monakhov, K. Y.; Rabu, P.; Robert, V. *Organometallics* **2012**, *31*, 4102–4105.
- (24) Hashimoto, T.; Urban, S.; Hoshino, R.; Ohki, Y.; Tatsumi, K.; Glorius, F. *Organometallics* **2012**, *31*, 4474–4479.
- (25) Zhang, Q.; Xiang, L.; Deng, L. *Organometallics* **2012**, *31*, 4537–4543.
- (26) Mo, Z.; Zhang, Q.; Deng, L. *Organometallics* **2012**, *31*, 6518–6521.
- (27) Macomber, D. W.; Rogers, R. D. *Organometallics* **1985**, *4*, 1485–1487.
- (28) Delgado, S.; Moreno, C.; Macazaga, M. J. *Polyhedron* **1991**, *10*, 725–729.
- (29) Simms, R. W.; Drewitt, M. J.; Baird, M. C. *Organometallics* **2002**, *21*, 2958–2963.

- (30) Gibson, S. E.; Johnstone, C.; Loch, J. A.; Steed, J. W.; Stevenazzi, A. *Organometallics* **2003**, *22*, 5374–5377.
- (31) van Rensburg, H.; Tooze, R. P.; Foster, D. F.; Slawin, A. M. Z. *Inorg. Chem.* **2004**, *43*, 2468–2470.
- (32) Poulton, A. M.; Christie, S. D. R.; Fryatt, R.; Dale, S. H.; Elsegood, M. R. J.; Andrews, D. M. *Synlett* **2004**, 2103–2106.
- (33) Fooladi, E.; Dalhus, B.; Tilset, M. *Dalton Trans.* **2004**, 3909–3917.
- (34) Llewellyn, S. A.; Green, M. L. H.; Cowley, A. R. *Dalton Trans.* **2006**, 4164–4168.
- (35) Danopoulos, A. A.; Wright, J. A.; Motherwell, W. B.; Ellwood, S. *Organometallics* **2004**, *23*, 4807–4810.
- (36) Cowley, R. E.; Bontchev, R. P.; Duesler, E. N.; Smith, J. M. *Inorg. Chem.* **2006**, *45*, 9771–9779.
- (37) Liu, B.; Xia, Q. Q.; Chen, W. Z. *Angew. Chem., Int. Ed.* **2009**, *48*, 5513–5516.
- (38) Lu, Z.; Cramer, S. A.; Jenkins, D. M. *Chem. Sci.* **2012**, *3*, 3081–3087.
- (39) Liu, B.; Liu, X.; Chen, C.; Chen, C.; Chen, W. *Organometallics* **2012**, *31*, 282–288.
- (40) McGuinness, D. S.; Gibson, V. C.; Steed, J. W. *Organometallics* **2004**, *23*, 6288–6292.
- (41) Hu, X.; Meyer, K. *J. Am. Chem. Soc.* **2004**, *126*, 16322–16323.
- (42) Hu, X.; Castro-Rodriguez, I.; Meyer, K. *J. Am. Chem. Soc.* **2004**, *126*, 13464–13473.
- (43) Cowley, R. E.; Bontchev, R. P.; Sorrell, J.; Sarracino, O.; Feng, Y.; Wang, H.; Smith, J. M. *J. Am. Chem. Soc.* **2007**, *129*, 2424–2425.
- (44) Deng, L.; Bill, E.; Wieghardt, K.; Holm, R. H. *J. Am. Chem. Soc.* **2009**, *131*, 11213–11221.
- (45) Mo, Z.; Li, Y.; Lee, H. K.; Deng, L. *Organometallics* **2011**, *30*, 4687–4694.
- (46) Mo, Z.; Chen, D.; Leng, X.; Deng, L. *Organometallics* **2012**, *31*, 7040–7043.
- (47) Matsubara, K.; Sueyasu, T.; Esaki, M.; Kumamoto, A.; Nagao, S.; Yamamoto, H.; Koga, Y.; Kawata, S.; Matsumoto, T. *Eur. J. Inorg. Chem.* **2012**, *2012*, 3079–3086.
- (48) Jaynes, B. S.; Doerrer, L. H.; Liu, S.; Lippard, S. J. *Inorg. Chem.* **1995**, *34*, 5735–5744.
- (49) Hojilla Atienza, C. C.; Milsmann, C.; Lobkovsky, E.; Chirik, P. J. *Angew. Chem., Int. Ed.* **2011**, *50*, 8143–8147.
- (50) Jewson, J. D.; Liable-Sands, L. M.; Yap, G. P. A.; Rheingold, A. L.; Theopold, K. H. *Organometallics* **1998**, *18*, 300–305.
- (51) Au-Yeung, H. Y.; Lam, C. H.; Lam, C.-K.; Wong, W.-Y.; Lee, H. K. *Inorg. Chem.* **2007**, *46*, 7695–7697.
- (52) DuPont, J. A.; Coxey, M. B.; Schebler, P. J.; Incarvito, C. D.; Dougherty, W. G.; Yap, G. P. A.; Rheingold, A. L.; Riordan, C. G. *Organometallics* **2007**, *26*, 971–979.
- (53) Bowman, A. C.; Milsmann, C.; Bill, E.; Lobkovsky, E.; Weyhermüller, T.; Wieghardt, K.; Chirik, P. J. *Inorg. Chem.* **2010**, *49*, 6110–6123.
- (54) Monfette, S.; Turner, Z. R.; Semproni, S. P.; Chirik, P. J. *J. Am. Chem. Soc.* **2012**, *134*, 4561–4564.
- (55) van Rensburg, H.; Tooze, R. P.; Foster, D. F.; Otto, S. *Inorg. Chem.* **2007**, *46*, 1963–1965.
- (56) Holland, P. L.; Cundari, T. R.; Perez, L. L.; Eckert, N. A.; Lachicotte, R. J. *J. Am. Chem. Soc.* **2002**, *124*, 14416–14424.
- (57) Detrich, J. L.; Reinaud, O. M.; Rheingold, A. L.; Theopold, K. H. *J. Am. Chem. Soc.* **1995**, *117*, 11745–11748.
- (58) Ceulemans, A.; Dendooven, M.; Vanquickenborne, L. G. *Inorg. Chem.* **1985**, *24*, 1159–1165.
- (59) Bain, G. A.; Berry, J. F. *J. Chem. Educ.* **2008**, *85*, 532–536.
- (60) Cooke, J.; Lightbody, O. C. *J. Chem. Educ.* **2010**, *88*, 88–91.
- (61) *Crystal Clear*; Rigaku/MSI Inc., Rigaku Corp., The Woodlands, TX, 2005.
- (62) ABCSOR; Higashi, Rigaku Corporation, Tokyo, Japan, 1995.
- (63) Sheldrick, G. M. *SHELXTL97: Program for Refinement of Crystal Structures*; University of Göttingen: Göttingen, Germany, 1997.
- (64) Sheldrick, G. M. *Acta Crystallogr., Sect. A* **2008**, *A64*, 112–122.